DOI: https://doi.org/10.52756/10.52756/ijerr.2023.v31spl.011 ***Int. J. Exp. Res. Rev.*, Special Vol. 31: 108-118 (2023)**

Original Article | *Peer Reviewed* | *Open Access*

International Journal of Experimental Research and Review (IJERR)
© Copyright by International Academic Publishing House (IAPH)
ISSN: 2455-4855 (Online)
www.iaph.in

A 2.45 GHz high gain radio frequency energy harvesting system in the Internet of Thing applications

Pradeep Chindhi[1*], Rajani Hiriyur [2] and Geeta Kalkhambkar[3]

[1]Electrical Engineering Department, Sant Gajanan Maharaj College of Engineering, Mahagaon, Kolhapur, Maharashtra, India; [2]Electronics and Communication Engineering Department, Jain College of Engineering, Belagavi, Karnataka, India; [3]Electronics and Telecommunication Engineering Department, Sant Gajanan Maharaj College of Engineering, Mahagaon, Kolhapur 416503, Maharashtra, India

E-mail/Orcid Id:

PC, pradeepchindhi.4003@gmail.com, https://orcid.org/0000-0001-8729-984X; *RH,* hprajani2@gmail.com, https://orcid.org/0000-0001-8443-7485; *GK,* geetakalkhambkar@gmail.com, https://orcid.org/0000-0001-9698-6190

Article History:
Received: 17th May., 2023
Accepted: 27th Jun., 2023
Published: 30thJul., 2023

Keywords:
RF Energy Harvesting, Gain, Directivity, Efficiency, Rectenna

Abstract: To power dedicated ultra-low-power Internet of Things (IoT) devices, high-voltage electric power must be converted to low voltage, which causes losses. Radio Frequency (RF) energy harvesting allows for scavenging ultra-low RF power from nearby RF sources. This paper proposes a single-band RF Energy Harvesting System (RFEHS) for the self-sustainable IoT application. The proposed Square Microstrip Patch Antenna (SMPA) is designed, simulated, and verified using Mentor Graphics software simulations and Computer Simulation Technology Microwave Studio (CST MWS) 3D electromagnetic simulator. For the design and simulation of the rectenna (Antenna + Rectifier), Advance Design System (ADS) is used. The SMPA is fabricated on Rogers RT5880 substrate material having a dielectric constant of 2.2 and a substrate thickness of 2.5 mm. The SMPA peak gain and directivity of 6.81 dBi and 7.24 dBi, respectively, are recorded. The proposed SMPA has an approximately omnidirectional radiation pattern at 2.45 GHz. The SMPA is tested on Vector Network Analyzer (VNA) to validate simulated CST MWS Mentor Graphics results. A single-stage voltage multiplier circuit has been analyzed and discussed using vendor-defined (Murata) library components. The rectenna has a maximum RF to DC conversion efficiency of 65.17% and a DC output voltage of 3.4 V at 10 dBm RF input power and load resistance, R= 3 kΩ. A Transmission Line (TL) equivalent model is derived for the proposed SMPA.

Introduction

The wireless communication system is one of the most vital technologies for advancing economic growth and social progress worldwide (Bakkali et al., 2016). The development of telecommunications infrastructure is spreading over rural and isolated areas far from urban centre's. In 2021, around 15 billion mobile devices were used worldwide, compared to around 14 billion in 2020. As per the prediction, there will be 18.22 billion mobile devices worldwide, a rise of 4.2 billion compared to 2020 (Federica Laricchia, 2023). Many RF and microwave signals are everywhere around us, and some research aims to use them as a renewable, ecologically beneficial energy source. Energy harvesting is the general term for renewable energy that captures existing or underused energy. Five hundred billion devices are supposed to be internet accessible by 2030, as per Cisco's prediction. Each IoT device has sensors to collect data and interact with the internet across a network (Gartner, 2016). RFEHS has been considered a solution to provide a long-term or endless power supply for IoT nodes. In the existing scenario, batteries are used to power IoT nodes, which reduces their lifespan. RFEHS tries to decrease battery usage and unnecessary wiring in some cases. Gain, directivity, radiation pattern, and radiation efficiency are crucial performance parameters for RFEHS to enhance the RF-to-DC conversion efficiency. RFEH systems have been the subject of intensive research in

***Corresponding Author:** pradeepchindhi.4003@gmail.com

This work is licensed under a Creative Commons Attribution-NonCommercial-NoDerivatives 4.0 International License.

recent years to attain the highest RF-to-DC conversion efficiency. Wang et al. (2022) discuss a printed 3D tree-shaped antenna with a solar energy harvesting system functioning between 2.39 GHz to 2.52 GHz with a peak gain of 6.0 dBi. A dual-band two-feed line square microstrip antenna operating at 900 MHz and 1800 MHz and a single diode rectifier with an impedance matching network to power biomedical wireless devices is demonstrated (Ojha et al., 2022). A Dual-band inset feed spurious free square slot loaded antenna operating at 2.49 GHz and 3.73 GHz (WiMax) and single diode rectifier with L type impedance matching circuit operating at 2.4 GHz is presented in (Chindhi et al., 2022). A miniaturized modified inset feed microstrip antenna for RF energy harvesting and its Characteristics Mode Analysis (CMA) is reported (Chindhi et al., 2020), which operates in the WiMAX middle-frequency band. Ali et al. (2022) present an H and J shape radiating patch, optimized parasitic patch in the ground, and two-stage Villard voltage multiplier with an L-type impedance matching network operating at 2.4 GHz. A 293.2×142.6×1.5 mm wideband circular shape antenna array for RFEH is given (Thuy and Minh, 2021). As the RFEH system requires an antenna with higher gain and specific polarization characteristics (Kalkhambkar et al., 2022), a compact omnidirectional radiation characteristics cantor set fractal monopole antenna operating at 2.4 GHz and for the range of 5 GHz to 8.5 GHz for IoT application is presented. Multi-substrate (FR4-Air-FR4) large circular aperture shape patch antenna with an air gap technique increases the bandwidth and gain (Savitri et al., 2018). The RFEH system gets bulky due to the multi-substrate and large aperture. A 1×4 hexagonal slot antenna array with a Wilkinson power divider is experimented with to enhance the gain and power sensitivity (Zhang et al., 2018). 1×4 antenna array with Wilkinson power divider increases the design complexity of the RFEH system. Corner truncation helps to achieve antenna impedance matching to enhance gain and shifting of the resonance frequency to the desired location (Chindhi et al., 2022). At low-intensity RF energy, a metamaterial-based high-efficiency rectenna for RF-DC conversion was used (Fowler et al., 2022). An antenna with metamaterial and Electromagnetic Band Gap (EBG) gives a high gain and directional radiation (Naktong et al., 2021). RFEHS has powered up on-chip CMOS and MOSFET-based temperature sensors (Kamakshi et al., 2022; Lin et al., 2008; Jeong et al., 2014; Chindhi et al., 2023).

Motivation

The number of ultra-low-power IoT devices is increasing due to recent technological advancements, which adds to the difficulty of routine battery maintenance and replacement. The need of the hour is for self-sustaining sources to power ultralow power devices. The environment is rich in RF energy, which can be used to power ultra-low IoT devices that continuously consume very little energy. In RF energy harvesting, issues include harmonics, reflection loss, insertion loss, and the availability of commercial components present challenges.

Past researchers have reported rectenna systems using ideal components provided by the Advance Design System library, ignoring electronic components' practical limitations. This proposed work's novelty lies in using vendor-defined (Murata) library components for designing the rectenna system. Another scientific contribution is the design of a high gain, high directivity antenna with a smaller size compared to the past literature in the field of RFEH.

The paper is organized as follows: The proposed SMPA's design, simulation, and experimental validation are presented in Section 2. Rectenna's single-band RFEHS design and simulation are addressed in Section 3. The reported SMPA's equivalent circuit concept is illustrated in Section 4. Section 5 ends with the conclusion and then provides a list of references.

Materials & Methods

Figure 1 shows a block diagram representation of RFEHS; it mainly comprises of receiving antenna, an impedance matching circuit/network, a rectifier/voltage multiplier circuit, and a power management unit followed by a load. Various parameters must be considered for optimal RF to DC conversion efficiency when designing RFEHS for the receiving antenna, impedance matching network, and rectifier circuit. The various parameters that need to be considered are mentioned in Figure 1. A key consideration in the design of microstrip antennas is the choice of the appropriate substrate material and substrate thickness. An antenna designer must know the impact of changing substrate material and thickness to achieve high gain, directivity, and bandwidth. According to the transmission line theory, the antenna Length × Width should be 48 mm × 40 mm, and the substrate Length × Width should be 63 mm × 55 mm to achieve resonance at 2.45 GHz. Instead of a rectangular patch, a square patch of Length = Width= 40 mm and a square substrate of Length = Width= 80 mm is considered for design. The

DOI: https://doi.org/10.52756/10.52756/ijerr.2023.v31spl.011

purpose behind increasing the substrate dimensions larger than required is to increase the gain.

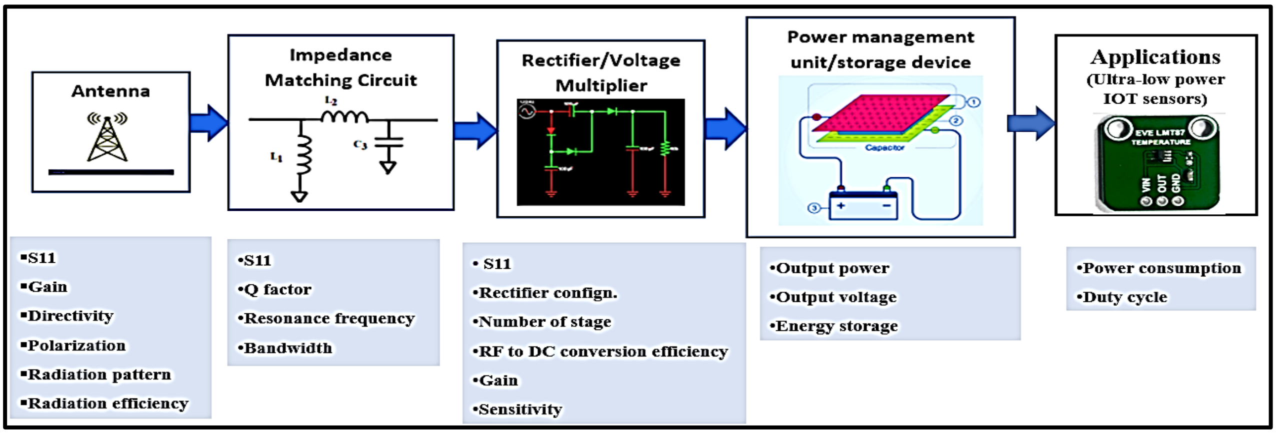

Figure 1. Block diagram of RFEHS

Results and Discussion

The proposed simulated and fabricated SMPA with inset line feed is revealed in Figure 2 and Figure 3, respectively. The geometry is optimized, and substrate details are given in Table 1 and Table 2. The simulated CST MWS, Mentor Graphics, and measured return loss (S11) of the proposed SMPA is in good agreement with acceptable deviation, as shown in Fig. 4 and Fig.5. The measured S11 of SMPA is found to be -38 dB at 2.50 GHz. An impedance of 46.18Ω (Z11), which is almost 50Ω, is seen at 2.45 GHz. The VSWR value below 2 in Figure 7 depicts the excellent matching of the antenna to its feed. Figure 6 shows the Radiation and Total efficiency of SMPA. In Figure 6, it is observed that the maximum Rad. and Tot. The efficiency of 89.77 % and 89.68 % are obtained. Figure 8 depicts the CST MWS and IE3D elevation plane radiation pattern of SMPA operating at 2.45 GHz with a main lobe magnitude of 6.81 dBi.

A transmission line model-derived antenna and a modified MSPA are compared regarding gain. A 25% gain improvement has been reported at 2.4 GHz when substrate dimensions are increased from 63 mm × 55 mm to 80 mm × 80 mm. As seen in Figure 9, an increase in substrate length and width enhances the fringing fields and aids in beam concentration in the main lobe direction, enhancing gain

Table 1. Gometrical details of proposed antenna

Sr. No.	Antenna parameter	Dimension (mm)
1	W_g (Ground plane width)	80.00
2	L_g (Ground plane length)	80.00
3	W_s (Width of substrate)	80.00
4	L_s (Length of substrate)	80.00
5	W_P (Patch width)	40.00
6	L_P (Patch length)	40.00
7	L_f (Length of feedline)	28.00
8	W_f (Width of feedline)	3.00
9	I_d (Inset depth)	8.00
10	Ig (Inset gap)	1.00

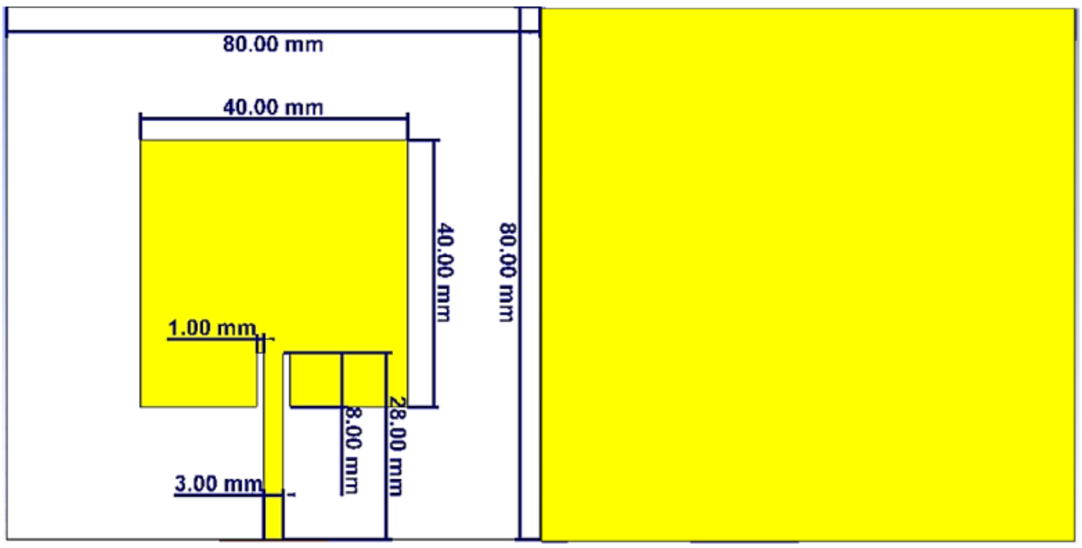

Figure 2. Simulated geometry of proposed SMPA (a) Top view (b) Ground plane

Figure 3. Fabricated antenna (a) Top view (b) Bottom view

Table 2. Substrate details

S. No.	Substrate parameter	Parameter details
1	Substrate material	Rogers RT5800
2	Dielectric constant	2.2
3	Loss Tangent	0.0009
4	Thickness of the Substrate	2.5 mm
5	Copper thickness	0.035µm
6	Copper conductivity	5.8e^ (+007)

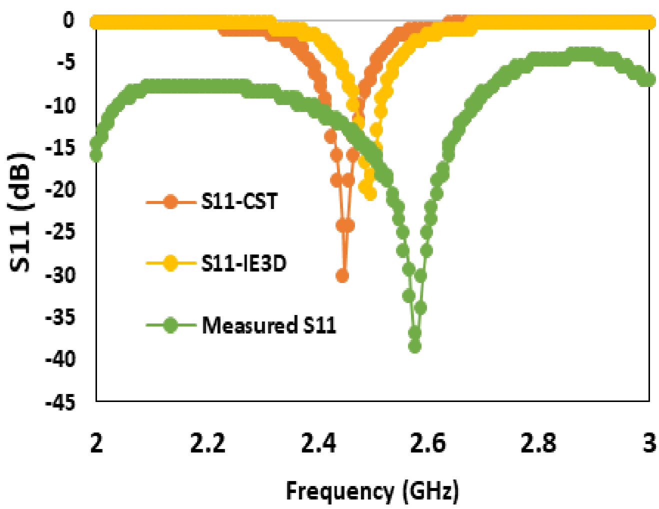

Figure 4. S11 of SMPA

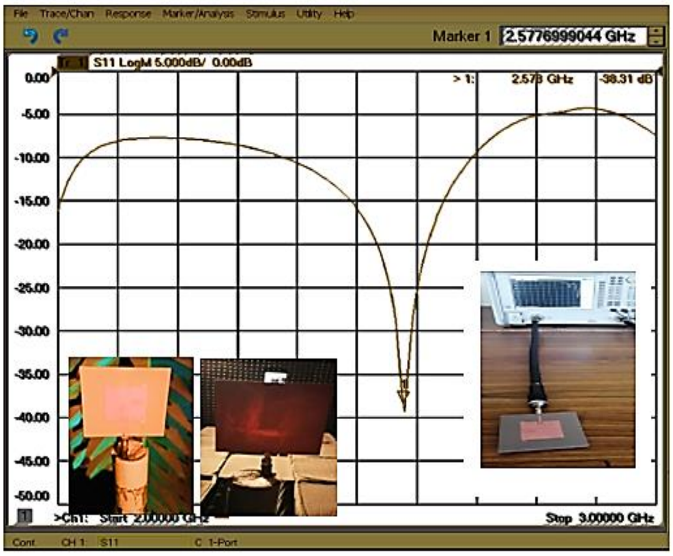

Figure 5. Measured S11 on VNA

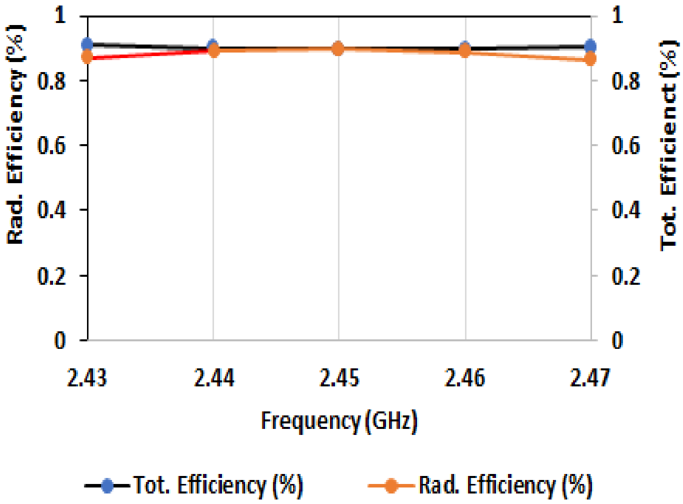

Figure 6. SMPA Rad. and Tot. efficiency

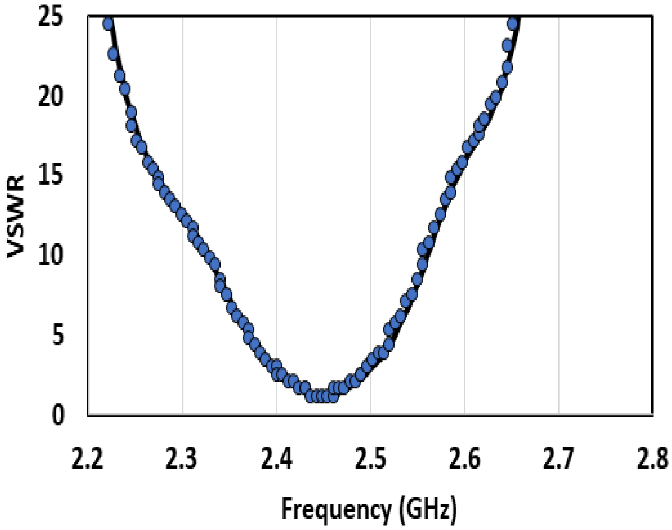

Figure 7. VSWR of SMPA

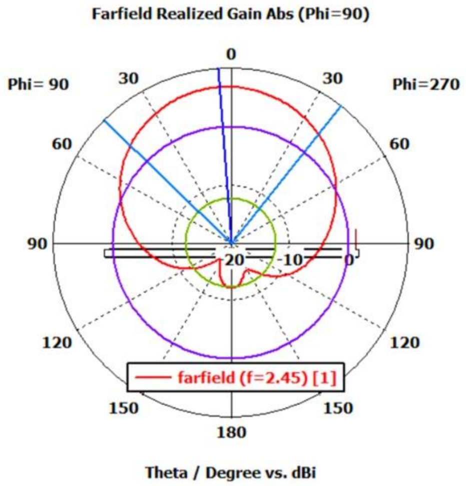

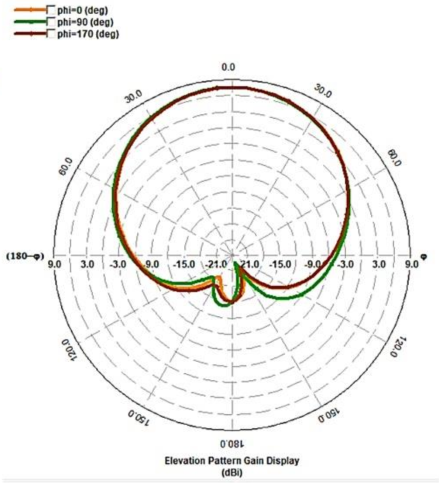

Figure 8. (a). Elevation plane radiation pattern in CST Figure 8 (b). Elevation plane radiation in Mentor Graphics

Radio Frequency Energy Harvesting System (RFEHS)

Figure 10 shows the RFEHS. It mainly consists of an RF energy source (Antenna), impedance matching network, and voltage doubler. The equations in (Pradeep Chindhi, et al., 2023) determine the required values for impedance-matching circuit components. As the impedance-matching circuit component's values obtained from the equations are ideal and are commercially unavailable, the nearest matching Murata library components values are selected, and the circuit has been simulated in ADS software. Impedance mismatch between the antenna and rectifier circuit causes reflections due to which the rectenna system experiences losses. An impedance matching network helps reduce the reflection losses at the expense of insertion losses of an impedance matching network; however, insertion losses are less significant at lower frequencies. In the case of higher frequencies and multistage voltage multiplier circuit, the effect of insertion losses are more significant and can be addressed by analyzing the quality factor of the impedance matching network (Hemour et al., 2014; Chen and Chiu, 2018; Lorenz et al., 2015; Wagih et al., 2021).

In Figure 10, the value of capacitor C8= 0.3 pF, L2= 3.9 nH, C4 and C5= 150 pF, respectively. Finally, load R1 is connected to the output of the voltage doubler. A zero-biased Agilent Technology (AT) high-frequency HSMS2850 diode is selected for the voltage doubler. Vender-defined library component capacitors and inductors (Murata) are selected for the impedance matching and voltage doubler circuit.

The return loss of an RFEHS is shown in Figure 11. The return loss of -18.0 dB at 2.42 GHz is observed. Figures 12 (a) to 12 (e) show the harvested power for fixed values of RF input power. The fixed values of RF input power are -20 dBm, -10 dBm, 0 dBm, 10 dBm, and 20 dBm, respectively. For a fixed value of input RF power, the load resistance R is swept from 1 kΩ to 5 kΩ. Figures 12 (d) and 12 (e) for 10 dBm and 20 dBm show that the DC power collected will be highest with a load resistance of 3kΩ.

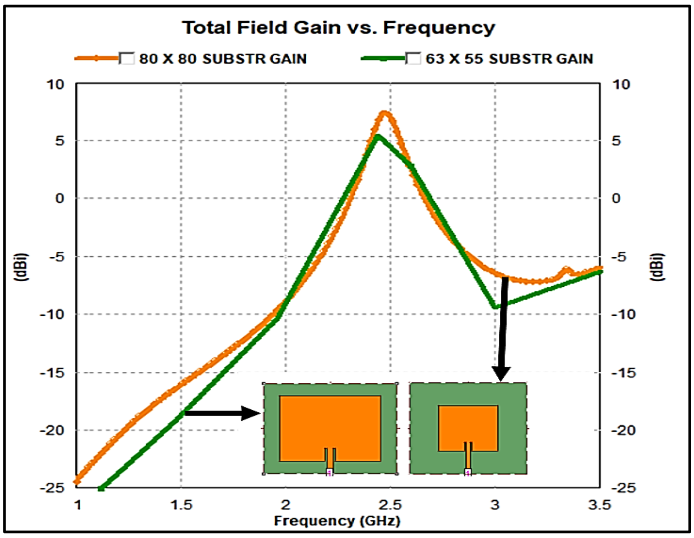

Figure 9. Gain comparison between transmission model dimensions (63 mm × 55 mm) and proposed SMPA (80 mm × 80 mm)

Figure 13 and Figure 14 show the output voltage Vs. Input RF power for the lower and higher load resistance R. The proposed RFEHS can provide a maximum of 3.40 V and 3.80 V at 10 dBm RF input power. Figure 15 (a) to 15 (d) shows the RF to DC conversion efficiency for the fixed value of load resistance R. The fixed value of load resistance R is 1kΩ, 2 kΩ, 3 kΩ, and 4 kΩ. Figure 15 (c) shows that for a fixed value of load resistance R= 3 kΩ, the maximum RF to DC conversion efficiency of 65.17 % is observed at 10 dBm RF input power. Figures 15 (a) to 15 (e) show that the proposed RFEHS gives the maximum RF to DC conversion when the load resistance is smaller than a higher value.

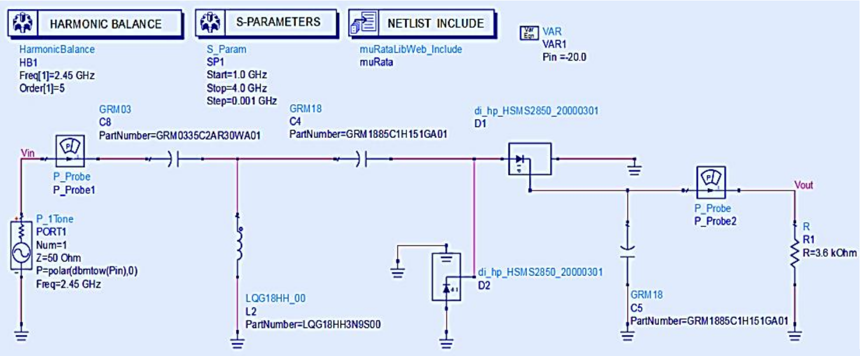

Figure 10. Rectenna system with vendor-defined (Murata) library components

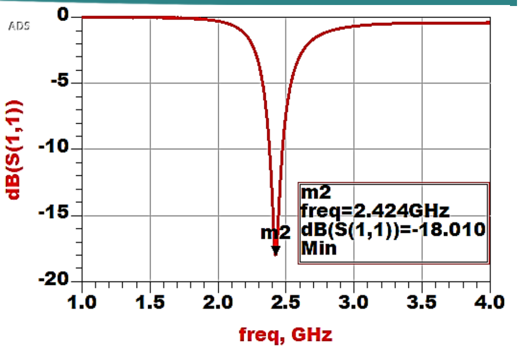

Figure 111. S11 of RFEHS

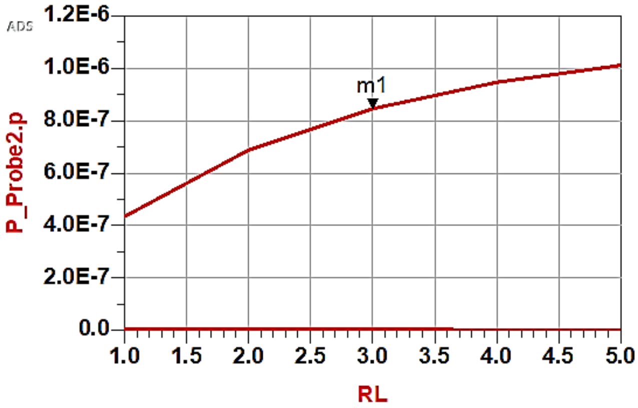

Figure 10. (a) Output power at -20 dBm

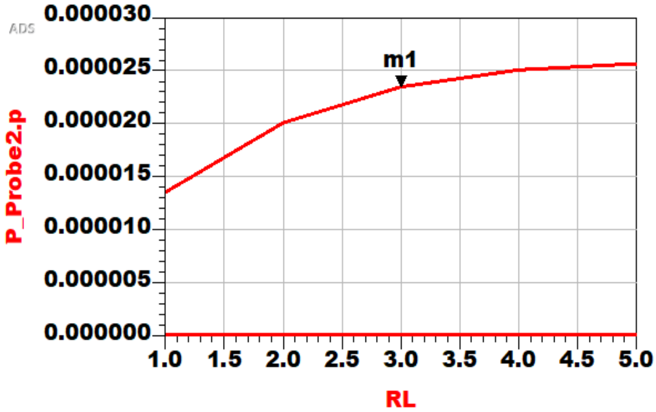

Figure 12. (b) Output power at -10 dBm

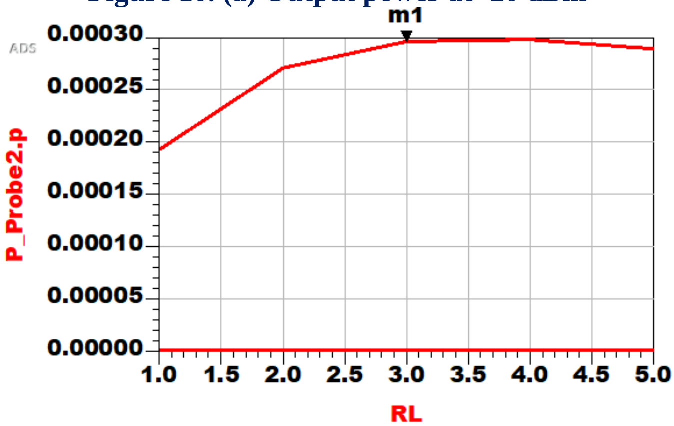

Figure 12. (c) Output power at 0 dBm

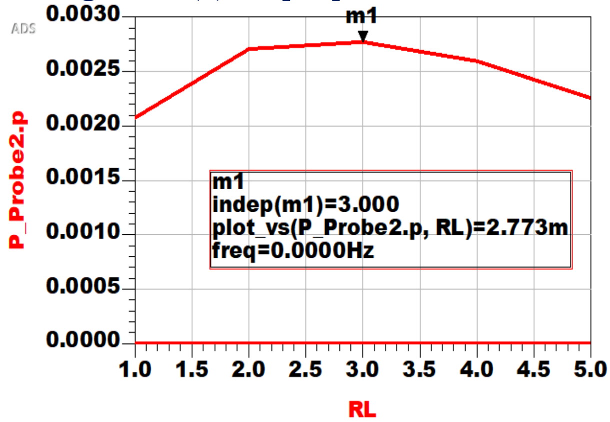

Figure 12 (d) Output power at 10 dBm

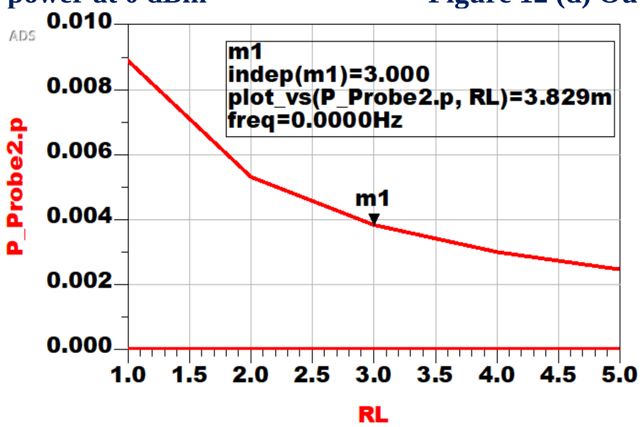

Figure 12. (e) Output power at 20 dBm

Figure 12. Output DC power against load resistance R for the received RF input power of (a) -20 dBm (b) -10 dBm (c) 0 dBm (d) 10 dBm and (e) 20 dBm

DOI: https://doi.org/10.52756/10.52756/ijerr.2023.v31spl.011

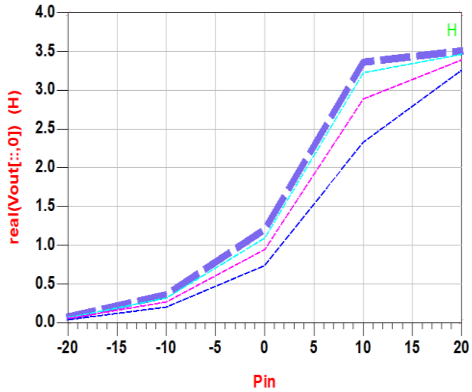

Figure 12. Vout Vs. Pin, for low load resistance, R

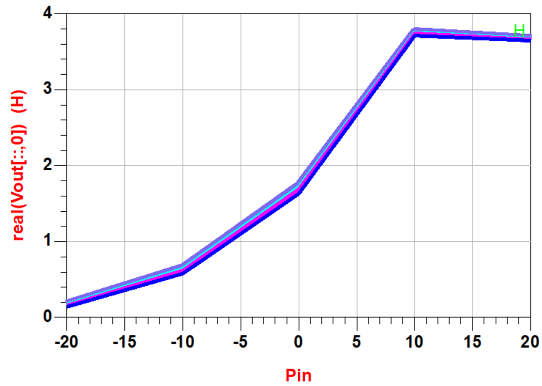

Figure 13. Vout Vs. Pin, for higher load resistance, R

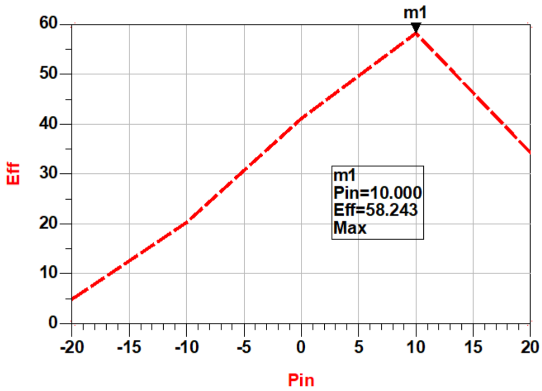

Figure 14. (a) Effi. Vs input power at 1 kΩ load

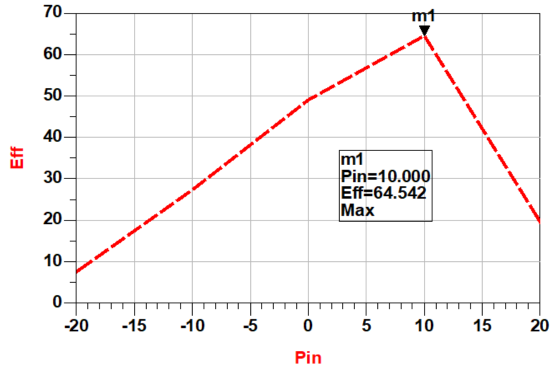

Figure 15. (b) Effi. Vs input power at 2 kΩ load

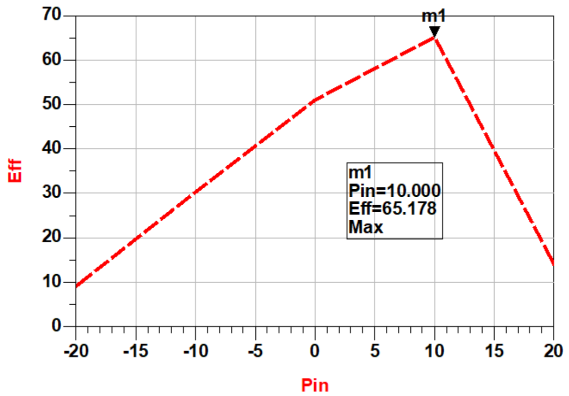

Figure 15. (c) Effi. Vs input power at 3 kΩ load

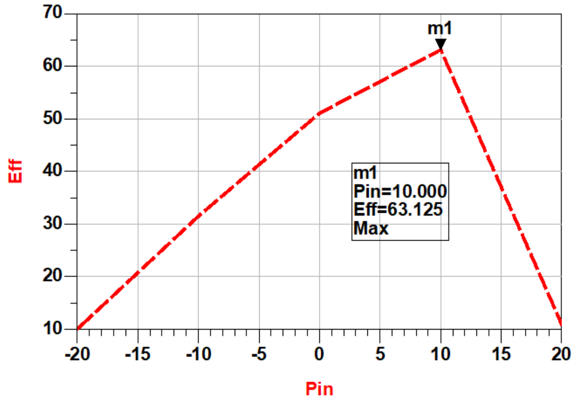

Figure 15. (d) Effi. Vs input power at 4 kΩ load

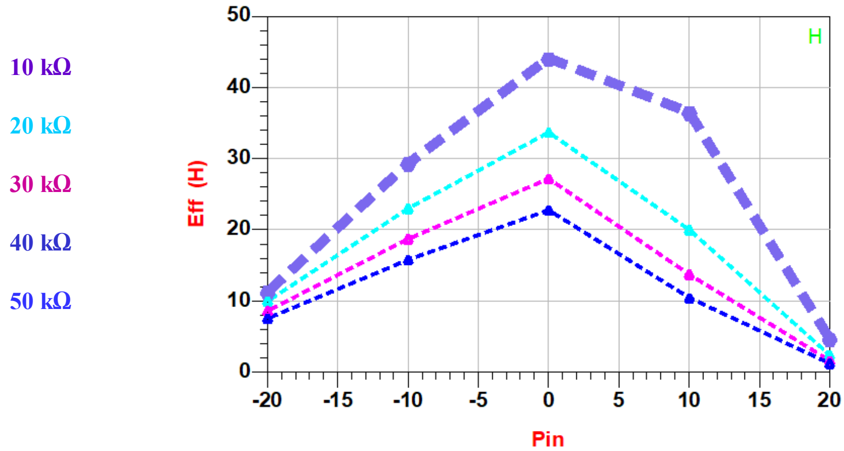

Figure 15 (e) Effi. Vs input power at higher load resistance

Figure 15. RF to DC conversion efficiecy againts RF input power for lower and higher load resistance R.

Table 3. Comparison with earlier studies

Ref.	Frequency (GHz)	Schottky diode/ MOSFET	Eff. (%) @ R	Output voltage (V)	Substrate material	Antenna gain (dBi)	Antenna size (mm)	Antenna details
Assogba et al., 2021	2.45	HSMS 2850	54 @ 1kΩ	0.73	FR-4	3.48	40×47.5×1.6	Rectangular slots loaded antenna
Pandey et al., 2021	2.42	HSMS 2813	78.53 @ 1kΩ	4.7	FR-4	3.94	80×80×0.67	Modified rectangular antenna
Benkalfate et al., 2022	2.45/5.2/8.2	Two MOSFET	77 @ 2 kΩ	0.11	Teflon glass	4.5	39×9×0.67	Flexible triangular antenna
Roy et al., 2023	2.4	HSMS 2850	49.5 @ 50 Ω	0.45	FR-4	3.35	240×200×1.6	DG* quad stub-loaded offset circular ring radiator
Said et al., 2019	2.45	02 Qty. HSMS 286B	Eff.=NR* @ R= 900 Ω	6.0 @ 30 dBm	FR-4	8.36	100×100×1.6	Two layers air-gap technology
Ojha et al., 2023	2.45	HSMS 2850	67.00 @ R= 2 kΩ	1.71	FR-4	3.35	80×90×1.6	DG hexagonal antenna
This Paper	**2.45**	**HSMS 2850**	**65.17 @ R= 3 kΩ**	**3.4**	**Rogers RT5880**	**6.81**	**80×80×2.5**	**Square microstrip antenna**

NR- Not Reported DG- Defective ground

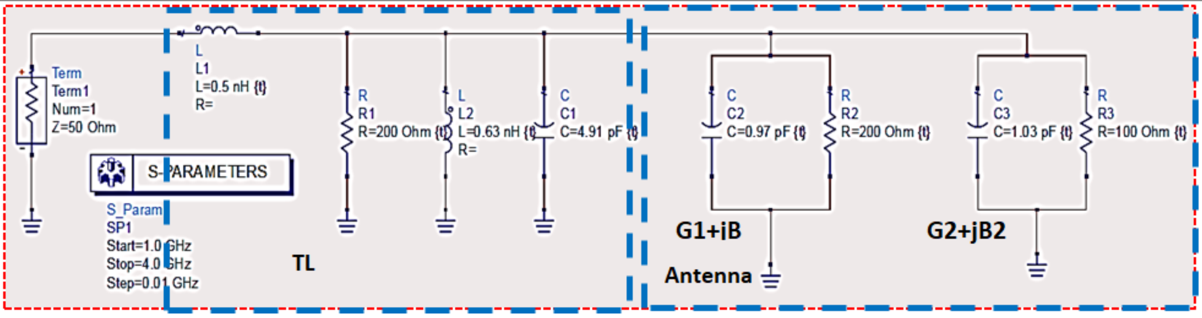

Figure 15. Equivalent circuit model of proposed microstrip patch antenna

Equivalate circuit model of SMPA

Microstrip antennas are the most commonly used form, as it is very easy to analyze with both transmission-line and cavity models. The transmission line model is the easiest (Mishra et al., 2018) The equivalent circuit values of the proposed SMPA could be precisely calculated using the following equations:

$$Y_1 = G_1 + jB_1 \ldots\ldots\ldots\ldots\ldots\ldots\ldots\ldots\ldots\ldots\ldots\ldots (1)$$

$$G_1 = \frac{W}{120\lambda_0}\left[1 - \frac{1}{24}(k_0 h)^2\right], \qquad \frac{h}{\lambda_0} < \frac{1}{10} \ldots\ldots\ldots\ldots (2)$$

$$B_1 = \frac{W}{120\lambda_0}\left[1 - 0.636 In(k_0 h)\right], \quad \frac{h}{\lambda_0} < \frac{1}{10} \ldots\ldots\ldots (3)$$

$$R_{in}(y = y_0) = \frac{1}{2(G_1 + G_{12})} cos^2\left[\frac{\pi}{L} y_0\right] \ldots\ldots\ldots\ldots\ldots\ldots (4)$$

$$G_{12} = \frac{1}{120\pi^2}\int_0^{\pi}\left[\frac{\sin\left(\frac{k_0 W}{2}cos\theta\right)}{cos\theta}\right]^2 J_0[k_0 Lsin\theta] sin^3\theta d\theta \ \ldots..(5)$$

Where, Y_1= Equivalent admittance, G_1=Conductance, B_1= Susceptance, W= Patch width, L= Patch length, h= Substrate hight, λ_0=Free-space wavelength, J_o= Bessel's function y_0= Inset feed lower distance, Rin=Input resistance.

Figure 16 and Figure 17 shows the optimized transmission line equivalent circuit model and return loss of the proposed SMPA. Again, an excellent agreement was found between simulated CST MWS, IE3D, and measured S11, S11 of RFEHS, and S11 of the transmission line model.

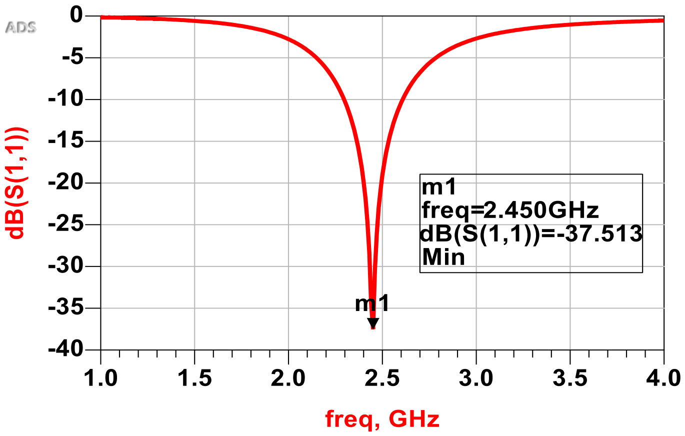

Figure 16. S11 of TL model

Comparison with earlier studies and related work

As shown in Table 3, the proposed work is compared with prior research in the field of RFEH at the frequency of 2.45 GHz in terms of efficiency, load resistance, voltage output, type of substrate material, type of Schottky diode/MOSFET, antenna gain, and overall size of the antenna. The proposed RFEHS outperforms the design presented in terms of output voltage (Assogba et al., 2021), RF to DC-conversion efficiency and antenna gain. The antenna size is small compared to the proposed design. The proposed design drives a load of 3 kΩ, whereas the design by Pandey et al. (2021) drives a load of 1 kΩ despite having higher efficiency. Benkalfate et al. (2022) have been optimized for miniaturization and efficiency. The output voltage is relatively low for ultralow power IoT devices. The design almost doubled the size of the intended antenna while reporting lesser efficiency and driving a smaller load of 50 Ω (Roy et al., 2023). With the airgap approach, the design reports a more significant gain, but it drives a smaller load with a higher input RF power and larger dimension (Said et al., 2019). The defective ground hexagonal antenna-based RFEHS presented gives slightly higher efficiency at the load of 2 kΩ. Ojha et al. (2023) the proposed RFEHS drives 3 kΩ load, which is higher compared to all other designs stated in table 3. The Rogers RT5880 substrate employed in the proposed RFEHS has high impedance stability, thermal stability, and minimal loss, allowing it to power loads up to 3 kΩ; the high gain of the SMPA allows for power harvesting over greater distances.

Conclusion

A single-band RFEHS is designed to power the wireless IoT sensor node. CST MWS is used for modelling and designing the intended SMPA. While designing and simulating a RFEHS and equivalent circuit model for the proposed SMPA was completed with ADS. The Rogers RT5880 material, which has a substrate thickness of 2.5 mm and an effective constant of 2.2, is used for fabricating SMPA. At 2.45 GHz peak gain, directivity, radiation efficiency, and total efficiency of 6.81 dBi and 7.24 dBi, 89.77 %, and 89.68% are attained. At 10 dBm RF input power and R= 3 kΩ the rectenna has a maximum RF to DC conversion efficiency of 65.17 % and DC output voltage of 3.4 V. For maximum RF energy harvesting with RFEHS, a high gain antenna without harmonics and a rectifier with low insertion loss are required, therefore, the suggested antenna with a rectifier (rectenna) meets the requirements of the RFEH system. This experimental work can be further enhanced to improve voltage output, power, and RFEHS conversion efficiency. The theoretical study with respective SMPA equivalent circuit implies that the S11 from the SMPA and its equivalent circuit match with higher accuracy. Increased substrate dimensions help improve the gain significantly up to the specific limit. The limitation of the study is increased substrate dimensions causing an increase in overall cost. However, this can be overcome with the help of specialized structures such as fractals and metamaterials.

Conflict of interest

None

References

Ali, W., Subbyal, H., Sun, L., & Shamoon, S. (2022). Wireless Energy Harvesting Using Rectenna Integrated with Voltage Multiplier Circuit at 2.4 GHz Operating Frequency. *Journal of Power and Energy Engineering*, *10*, 22-34. https://doi.org/10.4236/jpee.2022.103002.

Assogba, O., Mbodji, A.K., Diagne, S., Abdou Karim Diallo, A.K. (2021). Design of a Rectenna in 2.45 GHz Band Frequency for Energy Harvesting. *Energy and Power Engineering*, *13*(9), 333-342. https://doi.org/10.4236/epe.2021.139023.

Bakkali, A., Sebastia, J.P., Sogorb, T., Llario, V. & Escriva, A. (2016). A Dual-Band Antenna for RF Energy Harvesting Systems in Wireless Sensor Networks. *Journal of Sensors, 2016*, 5725836, https://doi.org/10.1155/2016/5725836.

Benkalfate, C., Ouslimani, A., Kasbari, A.E., & Feham, M. (2022). A New Compact Triple-Band Triangular Patch Antenna for RF Energy Harvesting Applications in IoT Devices. *Sensors. 22*(20), 8009. https://doi.org/10.3390/s22208009

Chen, Y.S., & Chiu, C.W. (2018). Insertion Loss Characterization of Impedance Matching Networks for Low-Power Rectennas. In IEEE Transactions on Components, Packaging and Manufacturing Technology, 8(9), 1632-1641. https://doi.org/10.1109/TCPMT.2018.2864183.

Chindhi, P., Rajani, H.P., & Kalkhambkar, G. (2022). A Spurious Free Dual Band Microstrip Patch Antenna for Radio Frequency Energy Harvesting. *Indian Journal of Science and Technology*, *15*(7), 266-275. https://doi.org/10.17485/IJST/v15i7.2025

Chindhi, P.S., Rajani, H.P., Kalkhambkar, G.B., & Khanai, R. (2020). Characteristics Mode Analysis of Modified Inset-fed Microstrip Antenna for Radio Frequency Energy Harvesting, *Biosc. Biotech. Res. Comm*., *13*(13), 171-176. https://doi.org/10.21786/bbrc/13.13/24

Chindhi, P., Rajani, H.P., & Kalkhambkar, G. (2023). Design and Optimization of Low-Cost RF Energy-Harvesting Circuit. Editors: S. Kannadhasan, R. Nagarajan, Alagar Karthick, Intelligent Technologies for Sensors Applications, Design, and Optimization for a Smart World. E-Book ISBN: 9781003314899.

Federica Laricchia (2023). Technology & Telecommunications› Forecast number of mobile devices worldwide from 2020 to 2025 (in billions). https://www.statista.com/statistics/245501/multiple-mobile-device-ownership-worldwide/

Fowler, C., Sinhara Silva, S., Thapa, G., & Zhou, J. (2022). High-efficiency ambient RF energy harvesting by a metamaterial perfect absorber. *Opt. Mater. Express.*, *12*, 1242-1250. https://doi.org/10.1364/OME.449494

Gartner (2016). Internet of Things At a Glance http://www.audentia-gestion.fr/cisco/pdf/at-a-glance-c45-731471.pdf

Hemour, S., Zhao, Y., Lorenz, C.H.P., Houssameddine, D., Gui, Y., Hu, C.M., & Wu, K. (2014). Towards Low-Power High-Efficiency RF and Microwave Energy Harvesting. *In IEEE Transactions on Microwave Theory and Techniques*, *62*(4), 965-976. https://doi.org/10.1109/TMTT.2014.2305134

Jeong, S., Foo, Z., Lee, Y., Sim, J., Blaauw, D., & Sylvester, D. (2014). A Fully-Integrated (2014). 71 nW CMOS Temperature Sensor for Low Power Wireless Sensor Nodes. *IEEE J. Solid-State Circuits*, *49*, 1682–1693. https://doi.org/10.1109/JSSC.2014.2325574

Kalkhambkar, G.B., Khanai,R., & Chindhi, P. (2022). Design and Characteristics Mode Analysis of a Cantor Set Fractal Monopole Antenna for IoT Applications. *Progress In Electromagnetics Research C*, *119*, 161-175. https://doi.org/10.2528/PIERC22012106

Kamakshi, D.A., Shrivastava, A., & Calhoun, B.H. (2016). A 0.2 V, 23 nW CMOS Temperature Sensor for Ultra-Low-Power IoT Applications. *J. Low Power Electron. Appl.*, *6*(2), 10. https://doi.org/10.3390/jlpea6020010

Lin, Y., Sylvester, D., & Blaauw, D. (2008) An ultra low power 1 V, 220 nW temperature sensor for passive wireless applications. In Proceedings of the 2008 IEEE Custom Integrated Circuits Conference, San Jose, CA, USA, 21–24 September 2008, pp. 507–510.

Lorenz, C.H.P., Hemour, S., & Wu, K. (2015). Modeling and influence of matching network insertion losses on ambient microwave power harvester. *IEEE, MTT-S International Conference on Numerical Electromagnetic and Multiphysics Modeling and Optimization* (NEMO), Ottawa, ON, Canada. pp. 1-3. https://doi.org/10.1109/NEMO.2015.7415051.

Mishra, B., Sing, V., & Singh, R. (2018). Gap Coupled Dual-Band Petal Shape Patch Antenna for WLAN / WiMAX Applications. *Advances in Electrical and Electronic Engineering*, *16*(2), 185-198. https://doi.org/10.15598/aeee.v16i2.2416

Naktong, W., Ruengwaree, A., Fhafhiem, N., & Krachodnok, P. (2021). Resonator Rectenna Design Based on Metamaterials for Low-RF Energy Harvesting. *Computers, Materials & Continua*, *68*(2), 1731-1750. https://doi.org/10.32604/cmc.2021.015843.

Pandey, R., Shankhwar, A.K., & Singh, A. (2021). Design and Analysis of Rectenna at 2.42 GHz for Wi-Fi Energy Harvesting. *Progress In Electromagnetics Research C*, *117*, 89-98. https://doi.org/10.2528/PIERC21100409

Ojha, S.S., Tomar, R.S., Akashe, S., Mishra, S., Dhakad, B., Sharma, M., Alqahtani, M.S., Ghoniem, R.M., Abbas, M., Soufiene, B.O. (2023). A

Broadband Rectenna for RF Energy Harvesting from Low Power Levels, PREPRINT (Version 1) available at Research Square. https://doi.org/10.21203/rs.3.rs-3002082/v1.

Roy, S., Jun-Jiat, I.T., Roslee, M.B., Saha, N., Kouzani, A.Z., Mahmud, P. (2023). A UWB Rectenna System Using a Defective Ground Structure (DGS) Monopole Antenna for Ambient Energy Harvesting. 2023, PREPRINT (Version 1) available at Research Square. https://doi.org/10.21203/rs.3.rs-3019576/v1

Said, M.A.M., Zakaria, Z., Husain, M.N., Misran, M.H., Noor, F.S.M. (2019). 2.45 GHz rectenna with high gain for RF energy harvesting. *TELKOMNIKA* (Telecommunication Computing Electronics and Control), *17*(1), 384. https://doi.org/10.12928/telkomnika.v17i1.11592

Savitri, I., Anwar, R., Amrullah, Y.S., Nurmantris, D.A. (2018). Development of Large Aperture Microstrip Antenna for Radio Wave Energy Harvesting. *Progress In Electromagnetics Research Letters*, *74*, 137-143. https://doi.org/10.2528/PIERL18030305

Shailendra Singh Ojha, P.K. Singhal, Vandana Vikas Thakare, (2022). Dual-band rectenna system for biomedical wireless applications. *Measurement: Sensors*, *24*, 100532. https://doi.org/10.1016/j.measen.2022.100532

Thuy, L.M., & Minh, D.Q. (2021). A Wideband Antenna Array for RF Energy Harvesting. *Journal of Military Science and Technology*, *72A*(5), 39-45. https://doi.org/10.54939/1859-1043.j.mst.72A.2021.39-45

Wagih, M., Weddell, A.S., & Beeby, S. (2021). Omnidirectional Dual-Polarized Low-Profile Textile Rectenna With Over 50% Efficiency for Sub-μW/cm2 Wearable Power Harvesting. *In IEEE Transactions on Antennas and Propagation*, *69*(5), 2522-2536. https://doi.org/10.1109/TAP.2020.3030992.

Wang, T., Huang, K., Liu, W., Hou, J., & Zhang, Z. (2022). A hybrid solar-RF energy harvesting system based on tree-shaped antenna array. *International Journal of RF and Microwave Computer-Aided Engineering*, *32*(10), e23301. https://doi.org/10.1002/mmce.23301.

Zhang, J., Bai, X., Han, W., Zhao, B., Xu, L., & Wei, J. (2018). The design of radio frequency energy harvesting and radio frequency-based wireless power transfer system for battery-less self-sustaining applications. *Int. J. RF Microw Comput. Aided Eng.*, *2018*, e21658. https://doi.org/10.1002/mmce.21658

How to cite this Article:

Pradeep Chindhi, Rajani Hiriyur and Geeta Kalkhambkar (2023). A 2.45 GHz high gain radio frequency energy harvesting system in the Internet of Thing applications. *International Journal of Experimental Research and Review*, *31*, 108-118.

DOI : https://doi.org/10.52756/10.52756/ijerr.2023.v31spl.011

This work is licensed under a Creative Commons Attribution-NonCommercial-NoDerivatives 4.0 International License.